Transient Electromagnetic Wave Propagation in Transverse Periodic Media

Karlsson, Anders; Kreider, Kevin

1994

CODEN:LUTEDX/(TEAT-7034)/1-22/(1994)

Transient Electromagnetic Wave Propagation in Transverse Periodic Media

Anders Karlsson and Kevin Kreider

Department of Electroscience
Electromagnetic Theory
Lund Institute of Technology
Sweden

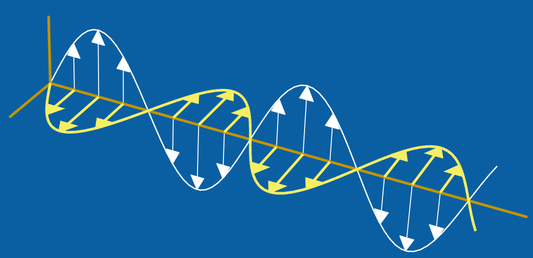

Anders Karlsson

Department of Electromagnetic Theory
Lund Institute of Technology
P.O. Box 118
SE-221 00 Lund
Sweden

Kevin Kreider

Department of Mathematical Sciences
University of Akron
Ohio 44325-4002
USA

Editor: Gerhard Kristensson

Abstract

In this paper, wave propagation of electromagnetic pulses in media that are periodic in one spatial direction is analyzed by a time domain technique. The special case of wave propagation in an inhomogeneous planar waveguide with perfectly conducting walls is also discussed. The wave equation is reduced to a set of one dimensional first order hyperbolic equations by an expansion in a complete set of basis functions and by utilizing a wave splitting technique. The method is especially useful for the propagation of broad pulses.

1 Introduction

The objective of this paper is to analyze pulse propagation in an infinitely wide medium that is periodic in the transverse direction, or equivalently, a waveguide with a variation of the permittivity in the transverse direction. For simplicity, only the propagation of TE (transverse electric) modes is discussed, since the wave equation is then scalar.

Ever since optical fibers have become important tools in transferring information, the analysis of wave propagation in inhomogeneous waveguides has received much attention. Much of this work deals with circular waveguides, even though both rectangular and planar optical waveguides are of interest in telecommunication [1]. A good overview of recent techniques and results can be found in books on optical waveguides, such as [2], [3] and [4]. These technqiues are often similar to those used in analyzing propagation through periodic media [5]. While most of the work on waveguides has been done in the frequency domain, several time-domain results, [6], [7], [8] and [9] for example, have appeared. In applications where pulses or finite wavetrains propagate through the waveguide, a time-domain analysis is relevant. In optical fibers, light pulses are finite wave trains of time-harmonic waves, but the beginning and ends of the pulses are transient. A detailed analysis of the propagation of these pulses must be based upon either a time-domain method or a method in the frequency domain which can handle a wide band of frequencies.

In the time domain method presented in this paper the wave equation for the waveguide is reduced to a one-dimensional problem by expanding the propagation speed $c(x)$ and the electric field in a complete set of basis functions. This approach has also been used in the frequency domain [1]. The time domain technique of wave splitting is applied to the one-dimensional wave equation: the wave field is split into left and right moving components. Since the medium is homogeneous in z, there is no coupling between the split fields. To describe the propagation of these fields, an operator, referred to as the propagator, is introduced. The propagator maps a split field from one position to another in the waveguide and is represented by a kernel satisfying a hyperbolic equation. The propagator is closely related to the scattering operators used in invariant imbedding techniques, cf [10], [11], [12], and to the operators used in the Green function approach [13]. The Green function approach has recently been applied to transient wave propagation in a homogeneous waveguide [7] and the present paper is partly based upon results in this paper.

The paper is organized as follows: Section 2 contains the statement of the problem under consideration. In Section 3, the wave equation is cast into the appropriate form for determining the electric field inside the waveguide. The internal field is represented by a propagation operation, described in Section 4, which allows for ease and flexibility in the numerical solution. The reflected field and the boundary condition at the end of the waveguide are presented in Section 5. Discretization of the equations and the algorithm for solving the direct problem are outlined in Section 6. Numerical results are presented in Section 7. Section 8 contains concluding remarks and plans for extending the results of this paper.

2 Problem statement

Physical Model. Consider a half-space, $z > 0$, which has a periodic variation of the material parameters in the x direction but no variation in the y and z directions. The half-space is attached at $z = 0$ to the homogeneous half-space $z < 0$, which has constant propagation speed $c_h = 1/\sqrt{\varepsilon_h \mu_0}$, where ε_h is the permittivity. The period in the x direction is p. In the analysis, the permittivity is assumed to be $x-$dependent, while the permeability is constant and there is no conductivity. These assumptions are not crucial for the analysis, but lead to a simple wave equation with no lower order terms. The formulation of the problem as a periodic halfspace problem may ultimately provide a means of examining more general wave propagation problems in three dimensions by wave splitting techniques.

The direct scattering problem under consideration is the following: an incident transverse electric wave $\boldsymbol{E}^i(x, z, t) = f(x, t - z/c_h)\hat{e}_y$, traveling in the $+z$ direction, impinges at the boundary $z = 0$ at time $t = 0$. The resulting reflected field and the internal field for $z > 0$ are to be calculated. Due to the geometry there is no coupling to the transverse magnetic mode so that

$$\boldsymbol{E}(x, z, t) = E(x, z, t)\hat{e}_y \tag{2.1}$$

everywhere. The periodicity of the geometry implies the conditions $E(x, z, t) = E(x + p, z, t)$ and $\partial_x E(x, z, t) = \partial_x E(x + p, z, t)$.

The equivalent waveguide problem is a wave guide of width p, homogeneous for $z < 0$ and with an $x-$dependent permittivity such that $\varepsilon(0) = \varepsilon(p)$ for $z > 0$. A special case of this waveguide is the familiar planar waveguide with perfectly conducting walls, in which case the walls are located at $x = 0$ and $x = a = \frac{p}{2}$, where the boundary conditions $E(0, z, t) = E(a, z, t) = 0$ are assumed. The incident wave in the homogeneous part of the waveguide is taken to be a waveguide mode. This important special case is discussed later in the paper.

Notes on Notation. All partial derivatives are indicated by ∂. Matrix or vector transposes are denoted by a superscript T. A superscript 'e' or 'o' indicates a coefficient associated with a cosine (even) or sine (odd) term. In the description of the matrix equation, k indicates the row (equation number) and n indicates the column (mode number within the series representations).

3 Problem Formulation

In this section, the wave equation is put into a form that is the basis for the introduction of the propagator. The electric field and propagation speed are written in terms of eigenfunction expansions, leading to a matrix formulation. Then the electric field is split into two components, which represent waves travelling along the + or − z-axis. The result is a first order system; its principle part is diagonalized, so that the unknowns correspond to the amplitudes of the modes that travel along the waveguide. Equation (3.34) is the main result of this section.

3.1 Matrix form of the wave equation

The internal electric field ($z > 0$) satisfies the wave equation

$$0 = \nabla^2 E(x,z,t) - \frac{1}{c^2(x)}\partial_t^2 E(x,z,t) \tag{3.1}$$

Since the geometry is periodic in x with a period p, it is appropriate to expand c^{-2} and E in terms of transverse eigenfunctions. In their most general form, the expressions read

$$c^{-2}(x) = \frac{a_0}{2} + \sum_{n=1}^{\infty} a_n \cos(\lambda_n x) + b_n \sin(\lambda_n x) \tag{3.2}$$

$$\begin{aligned} E(x,z,t) &= \frac{1}{2}E_0(z,t) + \sum_{n=1}^{\infty} E_n^e(z,t)\cos(\lambda_n x) + E_n^o(z,t)\sin(\lambda_n x) \qquad (3.3) \\ &= \sum_{n=0}^{\infty} \Psi_n(z,t) v_n(x) \end{aligned}$$

where $\{\lambda_n = 2n\pi/p, n = 0,1,2,\ldots\}$ is the set of eigenvalues, and Ψ_n and v_n are given by

$$\Psi_n : \quad E_0, E_1^e, E_2^e, \ldots, E_1^o, E_2^o, \ldots \tag{3.4}$$

$$v_n : \quad \tfrac{1}{2}, \cos(\lambda_1 x), \cos(\lambda_2 x), \ldots, \sin(\lambda_1 x), \sin(\lambda_2 x), \ldots \tag{3.5}$$

If the planar waveguide with perfectly conducting walls at $x = 0$ and $x = a = \frac{p}{2}$ is considered, then E loses its cosine terms, but the eigenvalues are the same.

Substitute these expansions into the wave equation and use the orthogonality of the eigenfunctions to obtain the coupled system of equations

$$0 = (\partial_z^2 - \lambda_0^2)E_0 - \frac{a_0}{2}\partial_t^2 E_0 - \frac{1}{2}\sum_{n=1}^{\infty} a_n \partial_t^2 E_n^e + b_n \partial_t^2 E_n^o \tag{3.6}$$

$$\begin{aligned} 0 &= (\partial_z^2 - \lambda_k^2)E_k^e - \frac{a_k}{2}\partial_t^2 E_0 - \frac{1}{2}\sum_{n=1}^{\infty}(a_{n-k} + a_{n+k} + a_{k-n} - a_0\delta_{nk})\partial_t^2 E_n^e \\ &\quad +(b_{n-k} + b_{n+k} - b_{k-n})\partial_t^2 E_n^o\,; \qquad k > 0 \end{aligned} \tag{3.7}$$

$$\begin{aligned} 0 &= (\partial_z^2 - \lambda_k^2)E_k^o - \frac{b_k}{2}\partial_t^2 E_0 - \frac{1}{2}\sum_{n=1}^{\infty}(a_{n-k} - a_{n+k} + a_{k-n} - a_0\delta_{nk})\partial_t^2 E_n^o \\ &\quad +(-b_{n-k} + b_{n+k} + b_{k-n})\partial_t^2 E_n^e\,; \qquad k > 0 \end{aligned} \tag{3.8}$$

These equations can be written in matrix form as

$$0 = \partial_z^2 \Psi(z,t) - T^2 \partial_t^2 \Psi(z,t) - \Lambda^2 \Psi(z,t) \tag{3.9}$$

where $\Psi = (\Psi_0, \Psi_1, \Psi_2, \ldots)^T$. Λ^2 is the diagonal matrix of squared eigenvalues associated with each component of Ψ:

$$\Lambda^2 = \begin{bmatrix} \lambda_0^2 & & & & & & \\ & \lambda_1^2 & & & & & \\ & & \lambda_2^2 & & & & \\ & & & \ddots & & & \\ & & & & \lambda_1^2 & & \\ & & & & & \lambda_2^2 & \\ & & & & & & \ddots \end{bmatrix} \tag{3.10}$$

T^2 is a symmetric matrix built exclusively from the coefficients in the expansion of $c^{-2}(x)$. T^2 is banded for a $c(x)$ whose expansion is finite, and is diagonal if $c(x)$ is constant. Nondiagonal elements of T^2 induce coupling among the modal coefficients in Ψ. It is expected that T^2 is a positive definite matrix so that its square root, denoted T, exists and is symmetric. While no proof of the existence of T has been found in general, for any specific problem it is easy to check numerically that all of the eigenvalues T^2, truncated to a finite size, are positive. Each eigenvalue of T (the square root of the eigenvalue of T^2) represents the inverse of the propagation speed of its corresponding mode. If the matrix T^2 is written as four submatrices, U^{ee}, U^{eo}, U^{oe} and U^{oo}, i.e.,

$$T^2 = \begin{pmatrix} U^{ee} & U^{eo} \\ U^{oe} & U^{oo} \end{pmatrix} \tag{3.11}$$

it is seen that

$$
\begin{aligned}
U^{ee}_{k0} &= U^{ee}_{0k} = \frac{1}{2} a_k; \quad k \geq 0 \\
U^{ee}_{kn} &= \frac{1}{2}(a_{n-k} + a_{n+k} + a_{k-n} - a_0 \delta_{n,k}); \quad k > 0,\ n > 0 \\
U^{eo}_{0n} &= U^{oe}_{n0} = \frac{1}{2} b_n; \quad n \geq 0 \\
U^{eo}_{kn} &= U^{oe}_{nk} = \frac{1}{2}(b_{n-k} + b_{n+k} - b_{k-n}); \quad k > 0,\ n > 0 \\
U^{oo}_{kn} &= \frac{1}{2}(a_{n-k} - a_{n+k} + a_{k-n} - a_0 \delta_{n,k}); \quad k > 0,\ n > 0
\end{aligned}
$$

As an example, for

$$
c^{-2}(x) = \frac{a_0}{2} + a_1 \cos(\lambda_1 x) + a_2 \cos(\lambda_2 x) + b_1 \sin(\lambda_1 x) + b_2 \sin(\lambda_2 x),
$$

and if the only modes retained in (3.3) are $n = 0, 1, 2, 3$, then the matrix T^2 has the form

$$
\frac{1}{2}\begin{bmatrix}
a_0 & a_1 & a_2 & 0 & b_1 & b_2 & 0 \\
a_1 & a_0 + a_2 & a_1 & a_2 & b_2 & b_1 & b_2 \\
a_2 & a_1 & a_0 & a_1 & -b_1 & 0 & b_1 \\
0 & a_2 & a_1 & a_0 & -b_2 & -b_1 & 0 \\
b_1 & b_2 & -b_1 & -b_2 & a_0 - a_2 & a_1 & a_2 \\
b_2 & b_1 & 0 & -b_1 & a_1 & a_0 & a_1 \\
0 & b_2 & b_1 & 0 & a_2 & a_1 & a_0
\end{bmatrix}
$$

3.2 Wave Splitting

The matrix equation (3.9) can be converted into a system of first order equations, hereafter called the dynamics, by splitting the electric field, and hence Ψ, into two components as follows:

$$
\Psi(z,t) = \Psi^+(z,t) + \Psi^-(z,t) \tag{3.12}
$$

$$
\Psi^\pm(z,t) = \frac{1}{2}(\Psi(z,t) \mp L \partial_z \Psi(z,t)) \tag{3.13}
$$

The operator L and the dynamics are found by the following formal calculations. First, write (3.9) in block matrix form:

$$
\partial_z \begin{bmatrix} \Psi \\ \partial_z \Psi \end{bmatrix} = \begin{bmatrix} 0 & I \\ T^2 \partial_t^2 + \Lambda^2 & 0 \end{bmatrix} \begin{bmatrix} \Psi \\ \partial_z \Psi \end{bmatrix} \tag{3.14}
$$

The first block row is an identity; the second block row is (3.9). Now, (3.13) can be written as

$$
\begin{bmatrix} \Psi^+ \\ \Psi^- \end{bmatrix} = \frac{1}{2} \begin{bmatrix} I & -L \\ I & L \end{bmatrix} \begin{bmatrix} \Psi \\ \partial_z \Psi \end{bmatrix} \tag{3.15}
$$

with formal inverse

$$\begin{bmatrix} \Psi \\ \partial_z \Psi \end{bmatrix} = \begin{bmatrix} I & I \\ -L^{-1} & L^{-1} \end{bmatrix} \begin{bmatrix} \Psi^+ \\ \Psi^- \end{bmatrix} \tag{3.16}$$

Combining these equations yields

$$\begin{aligned} \partial_z \begin{bmatrix} \Psi^+ \\ \Psi^- \end{bmatrix} &= \frac{1}{2} \begin{bmatrix} I & -L \\ I & L \end{bmatrix} \begin{bmatrix} 0 & I \\ T^2\partial_t^2 + \Lambda^2 & 0 \end{bmatrix} \begin{bmatrix} I & I \\ -L^{-1} & L^{-1} \end{bmatrix} \begin{bmatrix} \Psi^+ \\ \Psi^- \end{bmatrix} \\ &= \frac{1}{2} \begin{bmatrix} -L^{-1} - L(T^2\partial_t^2 + \Lambda^2) & L^{-1} - L(T^2\partial_t^2 + \Lambda^2) \\ -L^{-1} + L(T^2\partial_t^2 + \Lambda^2) & L^{-1} + L(T^2\partial_t^2 + \Lambda^2) \end{bmatrix} \begin{bmatrix} \Psi^+ \\ \Psi^- \end{bmatrix} \end{aligned} \tag{3.17}$$

The operator L is determined by forcing this system to be diagonal, so that Ψ^+ and Ψ^- decouple. Setting the off-diagonal elements in (3.17) to zero yields $L^{-1} = L(T^2\partial_t^2 + \Lambda^2)$ so that $L = (T^2\partial_t^2 + \Lambda^2)^{-1/2}$ and

$$L^{-1} = (T^2\partial_t^2 + \Lambda^2)^{1/2} \tag{3.18}$$

The dynamics may now be written formally as

$$\partial_z \begin{bmatrix} \Psi^+ \\ \Psi^- \end{bmatrix} = \begin{bmatrix} -\sqrt{T^2\partial_t^2 + \Lambda^2} & 0 \\ 0 & \sqrt{T^2\partial_t^2 + \Lambda^2} \end{bmatrix} \begin{bmatrix} \Psi^+ \\ \Psi^- \end{bmatrix} \tag{3.19}$$

To determine the precise form of the square root operator, assume that

$$L^{-1} f(t) = T\partial_t f(t) + \int_0^t H(t - t') f(t')\, dt' = T\partial_t f(t) + H * f(t) \tag{3.20}$$

where $f(t)$ is a vector, H is a matrix depending only on t, and T is the square root of the matrix T^2. Notice the notation $*$ for the convolution. This notation is used throughout the paper. The lower integration limit is 0 since all fields are zero for negative times and the upper limit is t due to causality. Then

$$(T^2\partial_t^2 + \Lambda^2) f = \sqrt{T^2\partial_t^2 + \Lambda^2}\sqrt{T^2\partial_t^2 + \Lambda^2} f = (T\partial_t + H*)(T\partial_t + H*) f \tag{3.21}$$

Note that T and H do not commute. Integrate by parts to obtain the equation for H,

$$0 = \partial_t H(t) T + T\partial_t H(t) + H * H(t) \tag{3.22}$$

with initial condition given by

$$\Lambda^2 = H(0)T + TH(0) \tag{3.23}$$

There is no closed form solution for H unless the waveguide is homogeneous [7], but H may be numerically computed quite easily, as is shown in Section 6. The dynamics may now be written as

$$\partial_z \begin{bmatrix} \Psi^+ \\ \Psi^- \end{bmatrix} = \begin{bmatrix} -T\partial_t - H* & 0 \\ 0 & T\partial_t + H* \end{bmatrix} \begin{bmatrix} \Psi^+ \\ \Psi^- \end{bmatrix} \tag{3.24}$$

3.3 Diagonalized System

By applying a similarity transform to diagonalize T, the system (3.24) can be converted to one in which the components of the unknown vector represent the amplitudes of the travelling modes supported by the waveguide.

Diagonalize T in this way:

$$D = QTQ^T \tag{3.25}$$

where the columns of Q^T are the eigenvectors of T. The matrix D is diagonal; its components represent the inverses of the propagation speeds of the wavefronts of the travelling modes,

$$D_{kk} = \frac{1}{c_k} \tag{3.26}$$

Mode 0 is the fastest, with speeds decreasing with higher index ($c_0 > c_1 > \cdots > c_n > c_{n+1} > \cdots$). Note that c_0 does not represent the propagation speed in vacuum. Now, let

$$\begin{aligned} A^{\pm}(z,t) &= Q\Psi^{\pm}(z,t), \qquad A = A^+ + A^- && (3.27) \\ K(t) &= QH(t)Q^T && (3.28) \\ Y &= Q\Lambda^2 Q^T && (3.29) \end{aligned}$$

The equation for K is

$$0 = \partial_t K(t)D + D\partial_t K(t) + K * K(t) \tag{3.30}$$

with initial condition given by

$$Y = K(0)D + DK(0) \tag{3.31}$$

Since Y and D are symmetric it follows that $K(0)$ is symmetric. By integrating (3.30) in time, the following equation is obtained

$$K(0)D + DK(0) = K(t)D + DK(t) + \int_0^t K * K(t')dt' \tag{3.32}$$

where the left hand side is symmetric. Using the theory for Volterra equations, this equation is seen to be uniquely solvable. The solution can be obtained by an iteration scheme that starts with $K^0(t) = K(0)$, and with $K^i(t)$ being the solution to

$$K(0)D + DK(0) = K^i(t)D + DK^i(t) + \int_0^t K^{i-1} * K^{i-1}(t')dt' \tag{3.33}$$

At every step, the matrix $\int_0^t K^{i-1} * K^{i-1}(t')dt'$ is symmetric, so that $K^i(t)$ is a symmetric matrix for all i. Thus $K(t)$ is a symmetric matrix.

Now, left-multiply (3.24) by Q to obtain

$$\partial_z \begin{bmatrix} A^+ \\ A^- \end{bmatrix} = \begin{bmatrix} -D\partial_t - K* & 0 \\ 0 & D\partial_t + K* \end{bmatrix} \begin{bmatrix} A^+ \\ A^- \end{bmatrix} \tag{3.34}$$

This equation is in a form suitable for numerical solution. The matrix operator on the right hand side is fairly simple because the A^+ components are decoupled from the A^- components and K is symmetric. By diagonalizing the system, the characteristics gain physical significance – their slopes are the inverse propagation speeds of the waveguide modes – and the unknowns represent the amplitude of the modes. In Section 6, (3.34) is solved numerically using the propagator representation described in Section 4.

3.4 Planar waveguide with perfectly conducting walls: orthogonality of modes

A special case of the theory in the preceeding sections is the planar waveguide with perfectly conducting walls at $x = 0$ and $x = a = \frac{p}{2}$. The boundary conditions imply that the expansion of the electric field (3.3) contains only sine functions. Thus only the submatrix T^{oo} appears in (3.9). Also, for the unitary matrix Q (3.25), only the odd-odd submatrix, Q^{oo} appears. The electric field for the guided modes is thus constructed as

$$E(x, z, t) = \sum_{n=1}^{\infty} E_n^o(z, t) \sin \lambda_n x \tag{3.35}$$

If only modes traveling in the $+z$ direction are considered, it follows that

$$E_n^o(z, t) = \sum_{m=1}^{\infty} A_m^+(z, t) Q_{mn}^{oo} \tag{3.36}$$

Now define the waveguide mode $e_m^+(x, z, t)$ as

$$e_m^+(x, z, t) = \sum_{n=1}^{\infty} A_m^+(z, t) Q_{mn}^{oo} \sin(\lambda_n x) \tag{3.37}$$

The set of functions $\{e_m^+(x, z, t)\}_{m=1}^{\infty}$ is a complete orthogonal set of functions over the region $0 < x < a$. The completeness follows from the fact that the set $\{\sin \lambda_n x\}_{n=1}^{\infty}$ is a complete set over the region $0 < x < a$ for functions with homogeneous boundary conditions. The orthogonality is seen from the following relations

$$\begin{aligned}
&\int_0^a e_m^+(x,z,t)e_n^+(x,z,t)dx \\
&= \sum_{\ell=1}^{\infty} A_m^+(z,t)Q_{m\ell}^{oo} \sum_{k=1}^{\infty} A_n^+(z,t)Q_{nk}^{oo} \int_0^a \sin(\lambda_\ell x)\sin(\lambda_k x)\,dx \\
&= \sum_{\ell=1}^{\infty} A_m^+(z,t)Q_{m\ell}^{oo}Q_{n\ell}^{oo}A_n^+(z,t)\frac{a}{2} \\
&= (A_m^+(z,t))^2\frac{a}{2}\delta_{mn}
\end{aligned} \tag{3.38}$$

The energy flux per unit length through the waveguide for a mode that propagates in the $+z$ direction is obtained by integrating the Poynting vector, $\boldsymbol{S} = \boldsymbol{E}\times\boldsymbol{H}$, over the cross section. From Maxwell's equations, it is seen that

$$P(t) = \int_0^a \boldsymbol{S}\cdot\hat{z}dx = -\frac{1}{\mu_0}\int_0^a E(x,z,t)\int_0^t \frac{\partial E}{\partial z}(x,z,t')dt'dx$$

From the dynamics in (3.34), it is seen that

$$\partial_z e_n^+(x,z,t) = -d_n\partial_t e_n^+(x,z,t) - \sum_{m=1}^{\infty} K_{nm} * A_m^+(z,t)\sum_{\ell=1}^{\infty} Q_{n\ell}\sin(\lambda_\ell x) \tag{3.39}$$

and thus

$$P(t) = \frac{a}{2\mu_0}\sum_{n=1}^{\infty} d_n(A_n^+(z,t))^2 + \frac{a}{2\mu_0}\sum_{n=1}^{\infty}\sum_{m=0}^{\infty} A_n^+(z,t)\int_0^t (K_{nm} * A_m^+)(t')dt' \tag{3.40}$$

Notice that there is coupling between the modes in the expression for the energy flux even though the modes are orthogonal.

4 The propagation operator representation

The propagation operator, or propagator, $\mathcal{G}^{\pm}(q)$ is defined to be the operator that maps a field moving in the $+z$ direction from position $z > 0$ to position $z + q > 0$

$$A^+(z+q, t+q/c_0) = \mathcal{G}(q)A^+(z,t) \tag{4.1}$$

Here, t is measured in wavefront time, so $t = 0$ at position z when the wavefront first arrives at that position. Since the half-space $z > 0$ is homogeneous in z, the propagator depends only on q. It has the representation

$$A_n^+(z+q, t+q/c_0) = A_n^+(z, t+q(1/c_0 - 1/c_n)) + \sum_{m=0}^{\infty} G_{nm}(q,t) * A_m^+(z,t), \quad n \geq 0 \tag{4.2}$$

The first term on the right hand side corresponds to the part of A_n^+ present at position z that has propagated with speed c_n without coupling to the other modes. The other term corresponds to the contribution to A_n^+ from the coupling between modes. The fastest component of that term travels as an A_0^+ mode with speed c_0 that couples to A_n^+ at position $z+q$. The matrix $G(q,t)$ satisfies the boundary condition

$$G_{nm}(0,t)=0, \quad n,m\geq 0 \tag{4.3}$$

The representation, (4.2), describes the total electric field inside the waveguide; because the medium is homogeneous in z, there is no internal reflection to generate waves moving in the $-z$ direction. In addition, since the medium is homogeneous in z, the propagator satisfies the rule

$$\mathcal{G}(q_1+q_2)=\mathcal{G}(q_1)\mathcal{G}(q_2) \tag{4.4}$$

By applying this rule to (4.2), it is easy to see that the matrix kernel G_{nm} satisfies

$$\begin{aligned} G_{nm}(q_1+q_2,t) &= G_{nm}(q_1,t+q_2(1/c_0-1/c_n))+G_{nm}(q_2,t+q_1(1/c_0-1/c_m)) \\ &\quad +\sum_{\ell} G_{n\ell}(q_1,t)*G_{\ell m}(q_2,t) \end{aligned} \tag{4.5}$$

This equation is useful in numerical calculations – after computing G for $z\in[0,q]$, the field can determined for $z\in[0,nq]$ by repeated use of the formula.

Note that the inverse of the operator $\mathcal{G}(q)$ can be defined from (4.4). By putting $q_1=-q_2=q$ it is seen that

$$(\mathcal{G}(q))^{-1}=\mathcal{G}(-q) \tag{4.6}$$

The operator $\mathcal{G}(-q)$ has the representation given by (4.2) and its kernel $G(-q,t)$ is related to $G(q,t)$ by the resolvent equation (4.5).

Two independent equations can be derived for the matrix kernel G_{nm}, one describing the change in G_{nm} as the thickness q of the slab $[z,z+q]$ changes with z remaining constant, and the other describing the change in G_{nm} as the position of the slab changes, with the thickness remaining constant.

The first equation is obtained by differentiating (4.2) with respect to q. The q-derivative of the left hand side of (4.2) is

$$\frac{d}{dq}\left[A_n^+(z+q,t+q/c_0)\right]=\partial_z A_n^+(z+q,t+q/c_0)+\frac{1}{c_0}\partial_t A_n^+(z+q,t+q/c_0) \tag{4.7}$$

The partial z-derivative is eliminated by using the dynamic equation (3.24), giving

$$\begin{aligned} \tfrac{d}{dq}A_n^+(z+q,t+q/c_0) = &\left(\frac{1}{c_0}-\frac{1}{c_n}\right)\Big(\partial_t A_n^+(z,t+q(1/c_0-1/c_n)) \\ &+\sum_m G_{nm}(q,0)A_m^+(z,t)+\sum_m \partial_t G_{nm}(q,t)*A_m^+(z,t)\Big) \\ &-\sum_m K_{nm}(t)*A_m^+(t+q(1/c_0-1/c_m)) \\ &-\sum_{\ell}\sum_m K_{n\ell}*G_{\ell m}*A_m^+(t) \end{aligned} \tag{4.8}$$

The q-derivative of the right hand side of (4.2) reads

$$\frac{d}{dq}(\text{rhs}) = \left(\frac{1}{c_0} - \frac{1}{c_n}\right) \partial_t A_n(z, t + q(1/c_0 - 1/c_n)) + \sum_m \partial_q G_{nm} * A_m(t) \qquad (4.9)$$

Equating (4.8) and (4.9) yields

$$\begin{aligned} \partial_q G_{nm}(q,t) = & \left(\frac{1}{c_0} - \frac{1}{c_n}\right) \partial_t G_{nm}(q,t) \\ & - K_{nm}(t + q(1/c_0 - 1/c_m)) - \sum_\ell K_{n\ell} * G_{\ell m}(t) \end{aligned} \qquad (4.10)$$

with initial condition

$$\left(\frac{1}{c_0} - \frac{1}{c_n}\right) G_{nm}(q,0) = 0 \qquad (4.11)$$

The second equation for G_{nm} is obtained by differentiating (4.2) with respect to z. The derivation is analogous to the derivation of (4.10); it follows that

$$\begin{aligned} \left(\frac{1}{c_m} - \frac{1}{c_n}\right) \partial_t G_{nm}(q,t) &= K_{nm}(t + q(1/c_0 - 1/c_m)) - K_{nm}(t + q(1/c_0 - 1/c_n)) \\ &\quad + \sum_\ell (K_{n\ell} * G_{\ell m} - G_{n\ell} * K_{\ell m})(t) \end{aligned} \qquad (4.12)$$

with initial condition

$$\left(\frac{1}{c_n} - \frac{1}{c_m}\right) G_{nm}(q,0) = 0 \qquad (4.13)$$

Equations (4.10) and (4.12) along with initial conditions (4.11) and (4.13) and boundary condition (4.3) provide a complete description of the propagation of modes generated by an incident impulse. If the incident field is not an impulse, it can be inserted into the right hand side of (4.2) to determine the modes.

Some properties of G can be determined by examining the two equations together. First, by letting $n = m$ in (4.12), it is easy to see that

$$\sum (K_{n\ell} * G_{\ell n} - G_{n\ell} * K_{\ell n})(t) = 0 \qquad (4.14)$$

Since $K(t)$ is a symmetric matrix it follows that $G(t)$ is symmetric.

Second, combining the two initial conditions yields

$$G_{nm}(q,0) = 0, \quad (n,m) \neq (0,0) \qquad (4.15)$$

The initial condition for G_{00} is determined below.

Third, a propagation of singularities argument shows that G_{nm} has no discontinuities if $n \neq m$. Each diagonal element G_{nn} does have a discontinuity along its characteristic, $t = q(1/c_n - 1/c_0)$, induced by the source term $K_{nn}(t + q(1/c_0 - 1/c_n))$. The value of the jump along the line $t = q(1/c_n - 1/c_0)$ is found by subtracting (4.10) with $t^- = q(1/c_n - 1/c_0) - 0^+$ from the same equation with $t^+ = q(1/c_n - 1/c_0) + 0^+$. Then

$$\frac{d}{dq}[G_{nn}(q, q(1/c_n - 1/c_0))] = -K_{nn}(0) \tag{4.16}$$

where $[G_{nn}(q, q(1/c_n - 1/c_0))] = G_{nn}(q, t^+) - G_{nn}(q, t^-)$ denotes the jump. Thus

$$[G_{nn}(q, q(1/c_n - 1/c_0))] = -K_{nn}(0)q \tag{4.17}$$

Specifically, then, the initial condition for G_{00} is

$$G_{00}(q, 0^+) = -K_{00}(0)q \tag{4.18}$$

Finally, the time delays in the source terms in (4.10) and (4.12) are easily explained. The term $K_{nm}(t + q(1/c_0 - 1/c_m))$ represents a mode m source originating at point z that travels along the source characteristic to the point $z + q$, where it couples to observation mode n. The term $q(1/c_0 - 1/c_m)$ is, in wavefront time, the time lag at $z + q$ between the arrival of the source and the first arrival of any signal coming from z. The term $K_{nm}(t + q(1/c_0 - 1/c_n))$ represents a mode m source that originates at point z, immediately couples to observation mode n and travels along the observation characteristic n to the point $z + q$.

5 Boundary condition and reflected field

When an incident electric field E^i, travelling through the homogeneous region $z < 0$ with speed c_h, hits the waveguide boundary at $z = 0$, it generates a reflected field E^r and a transmitted field E^t. The reflected field propagates in the $-z$ direction in the manner described in [7]. The transmitted field at the boundary is used in Section 4 as the input field to the propagator representation ($A_m^+(z, t)$ in (4.2)).

In this paper, only the TE (transverse electric) polarization is considered. The boundary conditions at $z = 0$ are

$$E^i(0, t) + E^r(0, t) = E^t(0, t) \tag{5.1}$$

$$\partial_z E^i(0, t) + \partial_z E^r(0, t) = \partial_z E^t(0, t) \tag{5.2}$$

As before, let the incident field be a plane wave polarized along the y-axis, i.e. a TE-mode:

$$\boldsymbol{E}^i(z, t) = f(t - z/c_h)\hat{e}_y = \frac{1}{2}\Gamma_0^+(z, t)\hat{e}_y \tag{5.3}$$

The reflected and transmitted fields may be represented as

$$\boldsymbol{E}^r(x, z, t) = \left[\sum_{n=0}^{\infty} \Gamma_n^-(z, t)v_n(x)\right]\hat{e}_y \tag{5.4}$$

$$\boldsymbol{E}^t(x, z, t) = \left[\sum_{n=0}^{\infty} \Psi_n^+(z, t)v_n(x)\right]\hat{e}_y \tag{5.5}$$

where the Γ_n^- and Ψ_n^+ must be determined. The terms of E^r exist in $z < 0$ and correspond to the (uncoupled) TE-modes that can exist in a homogeneous planar waveguide. The terms of E^t correspond to the modes that exist in $z > 0$. These modes couple to each other as they travel in the $+z$ direction within the waveguide.

Boundary condition (5.1) yields directly

$$\begin{aligned} \Gamma_0^+(0,t) + \Gamma_0^-(0,t) &= \Psi_0^+(0,t) && (5.6) \\ \Gamma_n^-(0,t) &= \Psi_n^+(0,t) \quad n = 1,2,3,\ldots && (5.7) \end{aligned}$$

Once all the $\Psi_n^+(0,t)$ are known, these equations are used to determine the $\Gamma_n^-(0,t)$, which in turn are used with Kristensson's propagator [7] to give the reflected field at any point in $z < 0$:

$$\begin{aligned} \Gamma_n^-(z, t - z/c_h) &= \mathcal{G}^{(0)}[\Gamma_n^-(0,t)](z,t) \qquad (5.8) \\ &= \Gamma_n^-(0,t) + c_h \lambda_n z \int_0^t \frac{J_1\left(\lambda_n \sqrt{c_h^2(t-t')^2 - 2zc_h(t-t')}\right)}{\sqrt{c_h^2(t-t')^2 - 2zc_h(t-t')}} \Gamma_n^-(0,t')\, dt' \end{aligned}$$

where J_1 is the Bessel function of first order. Since these waves travel in the negative direction, Kristensson's z is replaced here with $-z$. For use below, denote Kristensson's splitting kernel $H^{(0)}$, with the diagonal matrix representation (cf (3.20))

$$H_{nm}^{(0)} = \delta_{nm} c_h \lambda_n J_1(c_h \lambda_n t)/t \qquad (5.9)$$

Note that $H_{00}^{(0)} = 0$ since $\lambda_0 = 0$.

Boundary condition (5.2), combined with the nondiagonalized dynamics (3.24) to remove z derivatives, gives

$$-\frac{1}{2c_h}\partial_t \Gamma_0^+(0,t) + \frac{1}{2c_h}\partial_t \Gamma_0^-(0,t) = -\frac{1}{2}\sum_{m=0}^{\infty} T_{0m}\partial_t \Psi_m^+(0,t) + H_{0m} * \Psi_m^+(0,t) \quad (5.10)$$

$$\begin{aligned} \frac{1}{c_h}\partial_t \Gamma_n^-(0,t) \quad &+ \quad H_{nn}^{(0)} * \Gamma_n^-(0,t) \qquad (5.11) \\ &= -\sum_{m=0}^{\infty} T_{nm}\partial_t \Psi_m^+(0,t) + H_{nm} * \Psi_m^+(0,t), \qquad n > 0 \end{aligned}$$

Equations for the $\Psi_m^+(0,t)$ are obtained by eliminating the Γ_n^- ($\Gamma_0^- = \Psi_0^+ - \Gamma_0^+$, $\Gamma_n^- = \Psi_n^+$ for $n > 0$), resulting in

$$\left(T^{(0)} + T\right) \partial_t \Psi^+(0,t) + \left(H^{(0)} + H\right) * \Psi^+(0,t) = U(t) \qquad (5.12)$$

with matrix $T^{(0)} = \dfrac{1}{c_h} I$ and vector $U(t) = ((2/c_h)\partial_t \Gamma_0^+(0,t), 0, 0, 0, \ldots, 0)^T$.

To obtain the form that is consistent with the diagonalized dynamics (3.24), apply the matrix Q on the left:

$$\left(T^{(0)} + D\right) \partial_t A^+(0,t) + \left(Q H^{(0)} Q^T + K\right) * A^+(0,t) = QU(t) \qquad (5.13)$$

or

$$S\partial_t A^+ + W * A^+ = B \tag{5.14}$$

The initial condition is

$$A^+(0,0) = 0 \tag{5.15}$$

The solution of (5.14) is discussed in Section 6.

6 Direct problem algorithm and discretization of equations

It is convenient to introduce dimensionless variables $z \leftarrow z/a$ and $t \leftarrow tc_h/a$, which corresponds to scaling a and c_h to one. These dimensionless variables are used in this and the following Section. The algorithm to solve the direct problem is:

1. Specify the incident plane wave as $E^i(x,0,t) = f(t) = \frac{1}{2}\Gamma_0^+(0,t)$.
2. Determine the effect of the boundary at $z = 0$ on the field by solving (5.14). This gives the reflected field in $z < 0$ ($\Gamma_n^-(0,t)$ in (5.8)) and the boundary condition for the internal field at $z = 0^+$.
3. Determine the propagator by solving (6.7), presented below, the discrete form of the propagator equation (4.10).
4. Determine the internal field by convolving the propagator with the boundary field at $z = 0^+$.

For the discretization of the equations that follow, set up the grid of points $(z_i, t_k) = (ih, kh)$, where h is chosen *a priori*, as shown in Figure 2.

6.1 Discretization of boundary condition equation

Equation (5.14) is discretized by combining the forward difference at t_{k-1} and the backward difference at t_k and approximating the convolution by the trapezoid rule to give

$$\begin{aligned} B_k + B_{k-1} &= \frac{2}{h}S(A_k^+ - A_{k-1}^+) \\ &\quad + \frac{h}{2}(W_0 A_k^+ + W_k A_0^+ + 2\sum_{n=1}^{k-1} W_{k-n} A_k^+) + (W * A^+)_{k-1} \end{aligned} \tag{6.1}$$

Subscripts denote evaluation at the indicated time step. Note that S is independent of time. Since $z = 0$, the only variable is t. This is rearranged to solve for A_k^+

assuming that W_k and all quantities at step $k-1$ (in particular, $(W*A^+)_{k-1}$) are known, as follows:

$$\begin{aligned}(2S+\tfrac{1}{2}h^2W_0)A_k^+ &= h(B_k+B_{k-1})+2SA_{k-1} \\ &\quad -\frac{1}{2}h^2W_kA_0^+ - h^2\sum_{n=1}^{k-1}W_{k-n}A_k^+ - h(W*A^+)_{k-1}\end{aligned} \tag{6.2}$$

The matrix $2S+\frac{1}{2}h^2W_0$ is independent of time, so with the initial condition $A_0^+=0$, the system is solved for all time steps by inverting the matrix once and iterating. The result is the vector of mode coefficients $A^+(0,t_k)$, $k=0,1,2,\ldots$, which are used in Step 4.

6.2 Discretization of K-matrix equation

Equation (3.30) is discretized using a forward difference at t_k to give

$$K_{k+1}D+DK_{k+1}=K_kD+DK_k-h(K*K)_k \tag{6.3}$$

Because D is diagonal, the standard algorithm for solving this type of matrix equation ([14], section 6.4) reduces the system to a set of decoupled equations, which are trivial to solve. The elements of K at time t_k are given by

$$K_{ij}(t_k)=\frac{C_{ij}(t_k)}{D_{ii}+D_{jj}} \tag{6.4}$$

with

$$C_k=K_{k-1}D+DK_{k-1}-h(K*K)_{k-1} \tag{6.5}$$

Equation (6.4) is iterated over time index k starting with the discretized initial condition

$$K_{ij}(0)=\frac{Y_{ij}}{D_{ii}+D_{jj}} \tag{6.6}$$

6.3 Discretization of propagator equation

Equation (4.10) is solved numerically by adding the forward difference at point B $(z_{i-1},t_k-h/c_n)$ (indicated in Figure 2) and the backward difference at point A (z_i,t_k). These points lie on a line parallel to characteristic n, so B is not generally a grid point, necessitating the use of linear interpolation. The system of discrete

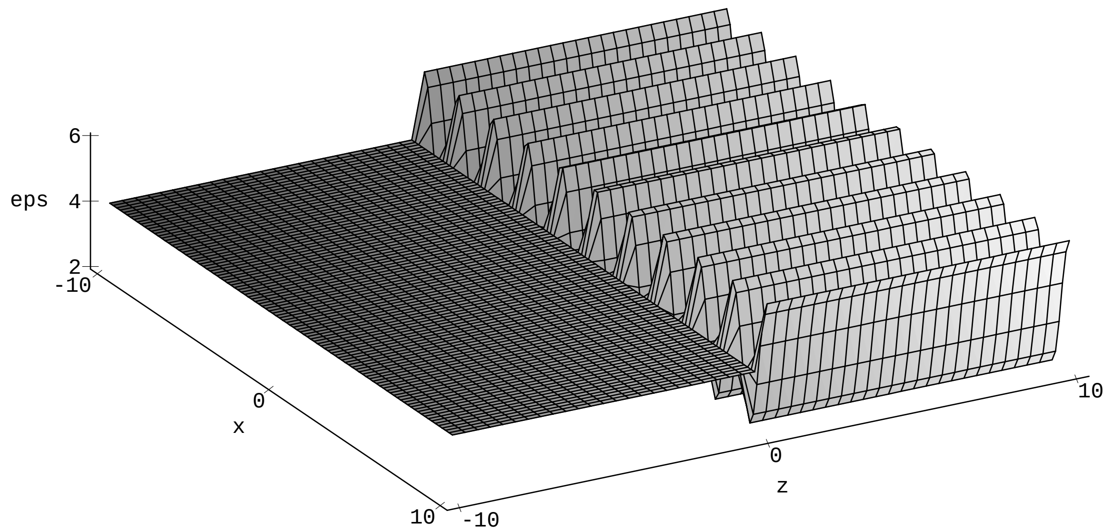

Figure 1: The geometry and permittivity profile. The incident field approaches from the left, along the $+z$ axis.

equations is

$$\begin{aligned}
\frac{2}{h}G_{nm}(z_i,t_k) &= \frac{2}{h}G_{nm}(z_{i-1},t_k-h(1/c_n-1/c_0))-K_{nm}(t_k-z_i(1/c_m-1/c_0)) \\
&- K_{nm}(t_k+z_i/c_0-h/c_n-z_{i-1}/c_m)-h\sum_p\sum_{\ell=1}^{k-1}K_{np}(t_{k-\ell})G_{pm}(z_i,t_\ell) \\
&- \frac{h}{2}\sum_k[K_{nk}(t_k)G_{km}(z_i,0)+K_{nk}(0)G_{km}(z_i,t_k)] \\
&- \sum_k K_{nk}*G_{km}(z_{i-1},t_k-h(1/c_n-1/c_0)) \qquad (6.7)
\end{aligned}$$

It is awkward to write these equations in matrix form because the time delays in the source term vectors are different for each component, but the system is straightforward to solve.

7 Numerical Examples

In the first part of this section, some general aspects of the numerical calculations are discussed. Then an explicit numerical example is presented together with several figures.

The main part of the numerical calculation is the calculation of the splitting matrix $K(t)$ and the propagator $G(z,t)$. The computation of K is virtually instantaneous, while the computation of G is considerably more time-consuming.

The matrix K is an analog of Kristensson's propagation kernel given in (5.9). Although no explicit expression for the matrix element $K_{nm}(t)$ is known, each el-

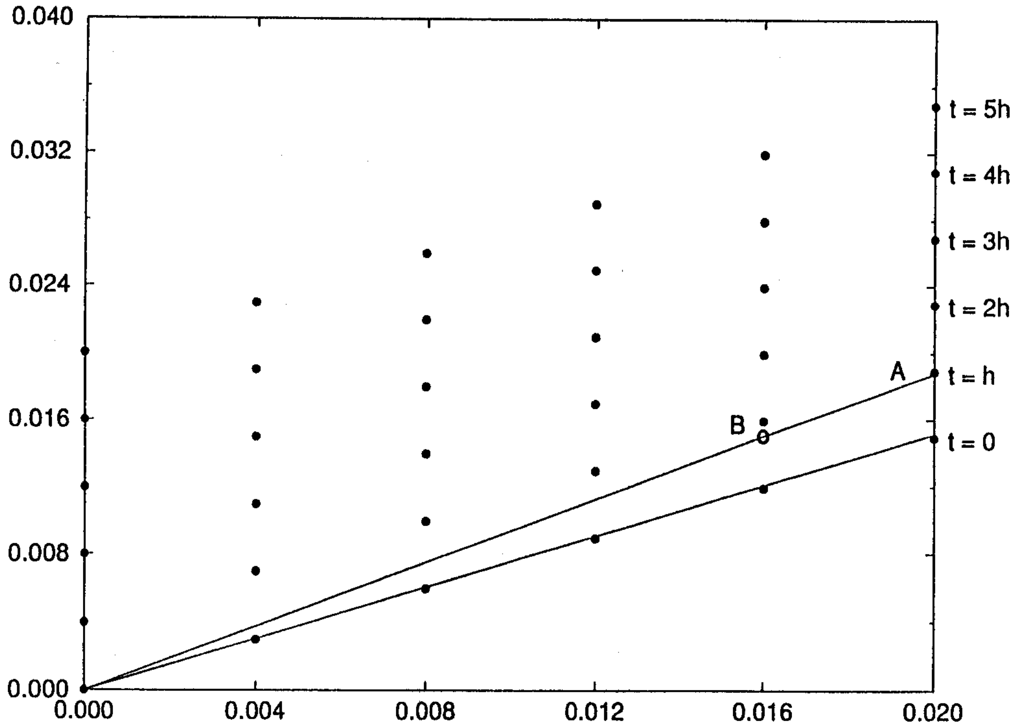

Figure 2: The grid. Solid dots represent the grid points (z_i, t_j), $i, j = 0, \ldots, N$. The lines represent the characteristics for the two fastest modes. The hollow dot is the interpolation point used in (6.7).

ement exhibits behavior similar to Kristensson's kernel $(J_1(\tau)/\tau)$, cf (5.8)). The closer $c(x)/c_h$ is to 1, the more diagonally dominant K is.

Generally, the size of the truncated matrix kernel G has to increase with depth into the medium. The reason for this is that since G is the response from a delta pulse, all frequencies are represented and infinitely many modes can propagate. As the delta pulse propagates through the medium, more and more power is transferred to the higher modes, which need to be included in G. However, due to computer memory limitations, it is impractical for G to be too large.

It is convenient to assume an incident pulse at $z = 0$ that is regular in the sense that its Fourier transform is neglibly small for sufficiently high frequencies. Then, the incident pulse gives rise to only a finite number N of propagating modes. The matrix kernel G can then be truncated to $N \times N$, and calculated as far into the medium as the desired accuracy will allow. Next, the field at this depth (call it $z = q$) can be calculated using (4.2) with (5.3) as the input. Because the waveguide is homogeneous in z, $G(q, t)$ is independent of position, so the field at $z = q$ can be considered the incident field for the slab $(q, 2q)$. Applying (4.2) again has the effect of propagating the field from $z = q$ to $z = 2q$. This process is repeated until

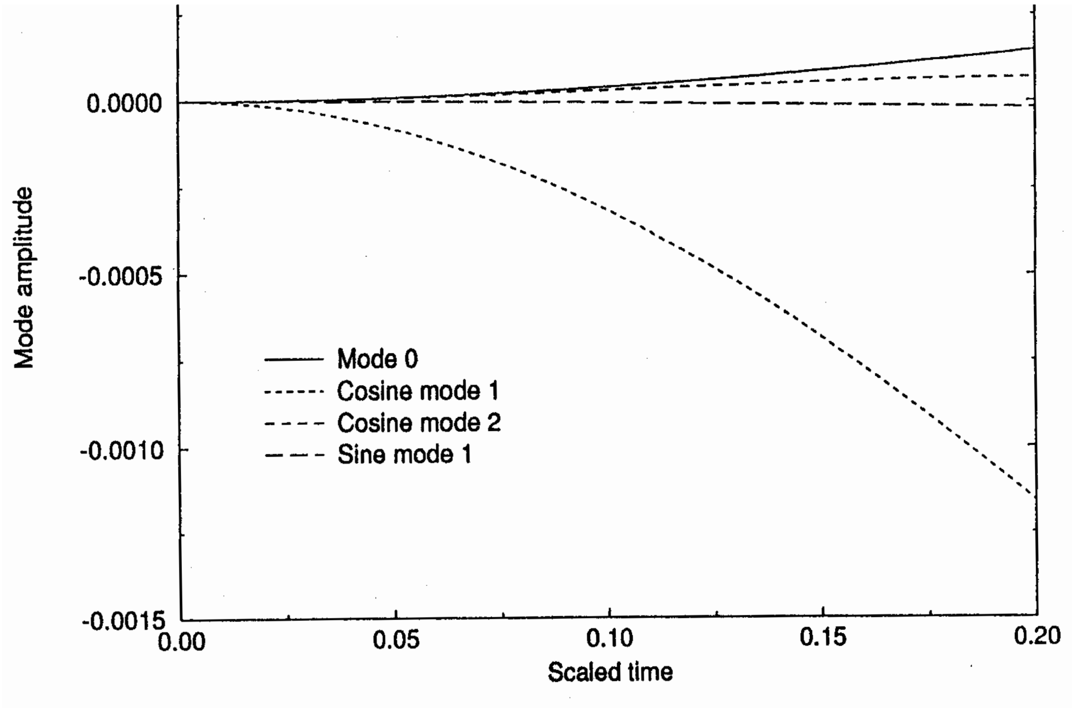

Figure 3: Reflected modes at the boundary $z = 0$. The other modes are essentially zero.

the field has been calculated at the required position. It is sufficient to truncate G to a size just slightly larger than the number of propagating modes induced by the incident pulse.

The example presented here is based upon the following profile for the normalized permittivity in the half-space $z > 0$

$$\frac{\varepsilon(x)}{\varepsilon_h} = \left(\frac{c_h}{c(x)}\right)^2 = 1 + .5\cos(\lambda_1 x) + .01\left(\cos(\lambda_2 x) + \sin(\lambda_1 x) + \sin(\lambda_2 x)\right) \quad (7.1)$$

As before, ε_h and c_h are the permittivity and the wavefront speed in the half-space $z < 0$. Thus there is a factor of 3 between the largest and smallest values of the permittivity in the profile, which can be considered to be quite strong. The incident field is a plane wave with dimensionless time behavior

$$\Gamma_0^+(0,t) = \frac{t^2}{2} \quad (7.2)$$

The Fourier transform of this field then falls off as $1/\omega^3$. Since the incident field is not very regular, it is expected that as z gets large, the truncation for the propagator matrix has to be large. The truncation for the matrices in the example is nmax $= 10$, which means that the matrix sizes are 21×21. The stepsize is $h = 0.002$ for both

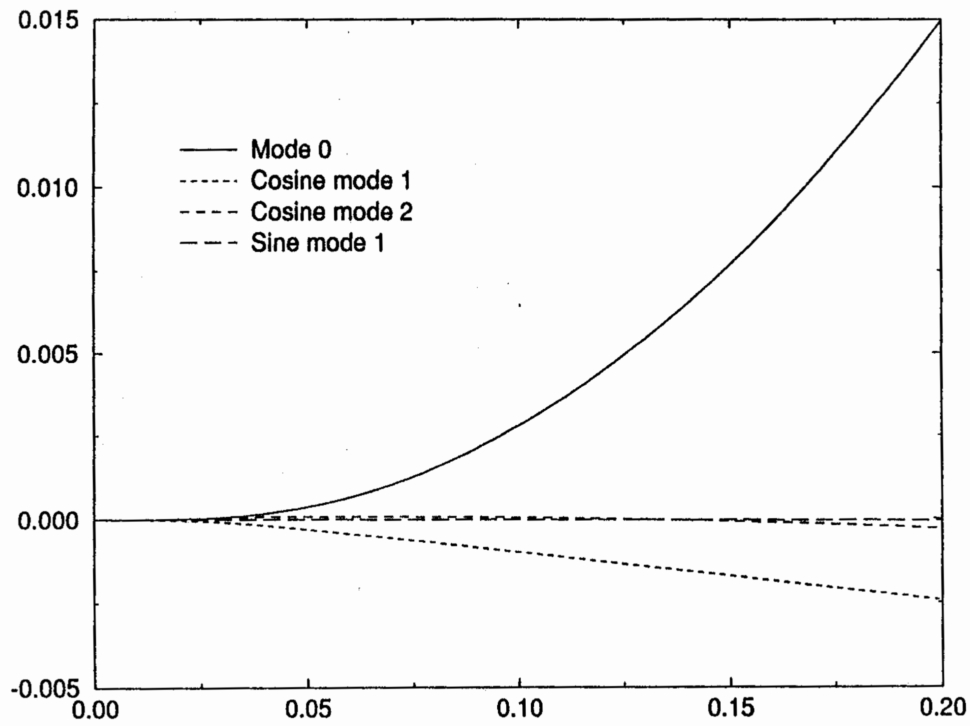

Figure 4: Transmitted modes at $z = .10$. The other modes are essentially zero.

t and z. The modes have been calculated for the first 100 steps, both in time and space. The propagator equation (4.10) has been solved from $z = 0$ to $z = 0.20$. On a fast workstation, such a computation takes on the order of 10 minutes. The truncation needed to compute G accurately at $z = .20$ is larger than that needed for $z = .10$, so it would be better to use the recursive method described above to calculate the field deeper in the medium; however, this has not been done in the examples.

In Figure 3, some of the reflected modes are presented. Notice that there is not much reflection into the fundamental mode Γ_0^-. The reason for this is that the mean values of the impedance in the two half-spaces $z < 0$ and $z > 0$ are the same. Most of the reflected energy is instead channeled into the first cosine mode Γ_1^-. This is not surprising since the coefficient in the $\cos(\lambda_1 x)$ term in the permittivity is large. Also, note that the coupling to the sine modes is weak, since the coefficients of the sine terms in the permittivity are small. The other modes are essentially zero. In Figure 3, the modes are shown only up to time $t = 0.20$. However, there is no problem in calculating the reflected modes for larger times.

Figure 4 shows the same modes that are shown at the boundary in Figure 3 at the position $z = .10$. The other modes are essentially zero. There is more coupling

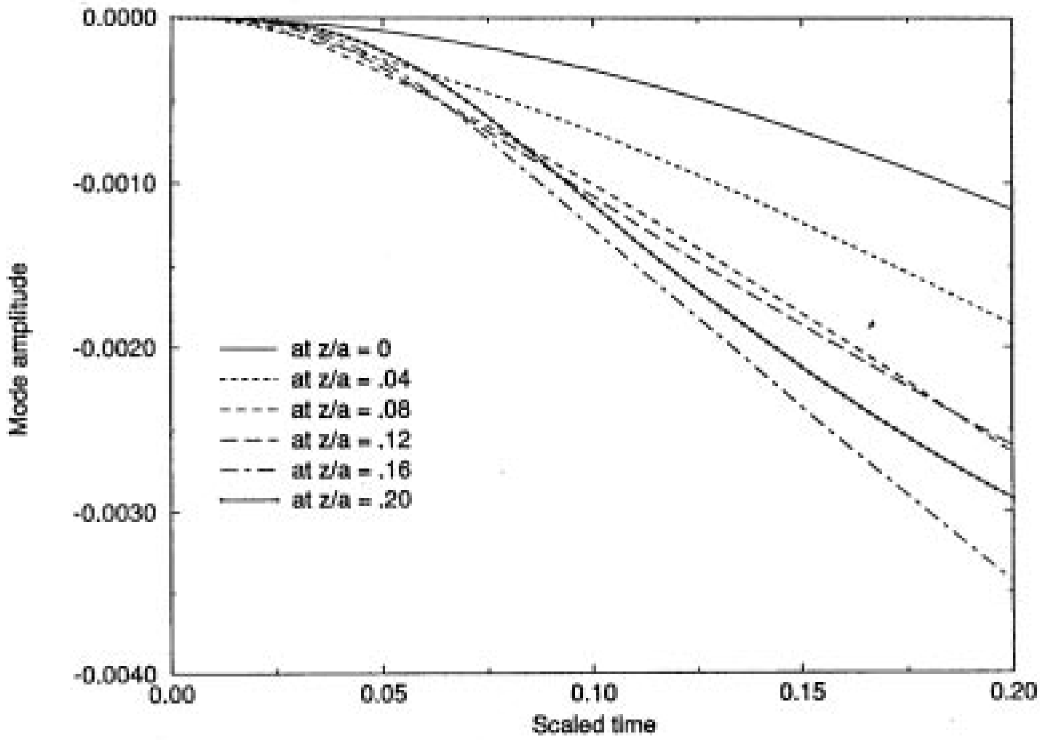

Figure 5: Cosine mode 1, $\Psi_1^+ = E_1^e$ in (3.3), at various depths.

to the higher modes here than at the boundary, and this coupling increases with depth into the medium. This fact is illustrated by the graphs in Figure 5, where the first cosine mode, $\Psi_1^+ = E_1^e$ in (3.3), is given at different depths. With a matrix truncation of nmax = 10 and the time behavior of the incident field, it seems that $z = .20$ is the largest value the algorithm can handle in this case without using the recursive method.

8 Conclusion

The propagation of an electric field along a waveguide that is homogeneous in depth but has a transverse variation in propagation speed is examined in the time domain. Expressions for the internal field and the reflected field are presented in terms of a propagation operator representation. Numerical results indicate that the method is practical.

The method can be extended to more complicated problems – direct problems include the study of waveguides with depth-dependent propagation speed $c(z, x)$, homogeneous waveguides with incident TM modes, waveguides with polar geometry, and media that are periodic in both x and y. Also, the inverse problems corresponding to these direct problems can be considered. Finally, by examining the formulation in the limit as the period goes to infinity, it may be possible to develop a wave splitting technique valid in three spatial dimensions.

References

[1] T. Rasmussen, et al, “Detailed Comparison of Two Approximate Methods for the Solution of the Scalar Wave Equation for a Rectangular Optical Waveguide,” *J. Lightwave Technol.* 19, 429-433 (1993).

[2] G. H. Owyang, *Foundations of Optical Waveguides*, Edward Arnold, London (1981).

[3] A. Snyder and J. Love, *Optical Waveguide Theory*, Chapman and Hill, London (1991).

[4] M. J. Adams, *An Introduction to Optical Waveguides*, Wiley, New York (1981).

[5] C. Elachi, “Waves in Active and Passive Periodic Structures: A Review,” *Proc. IEEE* 64, 1666-1698 (1976).

[6] M. Cotte, “Propagation of a pulse in a waveguide,” *Onde Elec.* 34, 143-146 (1954).

[7] G. Kristensson, “Transient Electromagnetic Wave Propagation in Wave Guides” Technical Report LUTEDX (TEAT-7026), Department of Electromagnetic Theory, P. O. Box 118, S-221 00 Lund, Sweden.

[8] W. P. Huang, S. T. Chu, A. Goss, S. K. Chaudhuri, “A scalar finite-difference time-domain approach to guided-wave optics,” *IEEE Photonics Technology Letters* 3, 524-526 (1991).

[9] W. P. Huang, S. T. Chu, S. K. Chaudhuri, “A semivectorial finite-difference time-domain method,” *IEEE Photonics Technology Letters* 3, 803-806 (1991).

[10] G. Kristensson and R. J. Krueger, “Direct and inverse scattering in the time domain for a dissipative wave equation. Part 1: Scattering operators,” *J. Math. Phys.* 27, 1667-1682 (1986).

[11] G. Kristensson and R. J. Krueger, “Direct and inverse scattering in the time domain for a dissipative wave equation. Part 2: Simultaneous reconstruction of dissipation and phase velocity profiles,” *J. Math. Phys.* 27, 1683-1693 (1986).

[12] G. Kristensson and R. J. Krueger, “Direct and inverse scattering in the time domain for a dissipative wave equation. Part 3: Scattering operators in the presence of a phase velocity mismatch,” *J. Math. Phys.* 28, 360-370 (1987).

[13] R. J. Krueger and R. L. Ochs, “A Green’s function approach to the determination of internal fields,” *Wave Motion* 11, 525-543 (1989).

[14] J. M. Ortega, *Matrix Theory*, Plenum Press, New York (1987).